



Montréal, Québec  
May 29 to June 1, 2013 / 29 mai au 1 juin 2013

## Comparison of the Chloride Permeability and Service Life Time Prediction Methods in Offshore Concrete Structures

Ahmed A. Abouhussien and Assem A. A. Hassan  
Memorial University of Newfoundland

**Abstract:** Offshore concrete structures are commonly subjected to high concentrations of chlorides which eventually lead to corrosion of the embedded reinforcing steel. The chloride permeability of concrete is the most significant factor affecting the onset of corrosion and the overall service life time of the structure. The purpose of this paper is to develop a relationship between rapid chloride permeability and chloride diffusion test results of different concrete samples. The tested concrete samples were subjected to ten alternative curing scenarios in hot, cold, and normal temperatures prior to testing. The developed relationship in this investigation was then exploited to predict the service life times of the tested concrete samples by means of the Fick's second law of diffusion. The investigation also included an accelerated corrosion test performed on counterpart samples in order to validate the predicted service life times obtained from the Fick's second law of diffusion. The recommendations of this paper can be of special interest to designers considering the use of reinforced concrete in offshore applications.

### 1. Introduction

Concrete in severe environments, such as that subjected to high percentages of chlorides, should be given a special design consideration to extend its service life. The reason behind this limitation is the increasing number of deteriorating structures due to concrete durability problems. Moreover, concrete structures in these environments are even deteriorating in a quicker rate. The most critical factor for this deterioration is the corrosion of embedded reinforcing steel. The corrosion requires the chlorides from deicing salts, groundwater, or seawater to penetrate the concrete cover and reach the reinforcing steel. Once the percentage of the chloride around the steel bar exceeds the threshold needed for corrosion initiation, the corrosion starts and followed by propagation through steel bars, which eventually leads to a mass loss and destruction of the concrete cover.

Chloride permeability is a significant property of the concrete representing its resistance to chloride ingress. Such property directly affects the time for chlorides to reach the reinforcing bars and consequently the corrosion initiation time. Most of the models used for corrosion prediction account for the resistance of concrete to chlorides (Boddy et al. 1999; Ehlen et al. 2009). Concrete with low permeability and dense microstructure proved to extend the time needed for corrosion to occur. In fact, the total service life time for the structures in marine environments can be increased using high performance or less permeable concretes (Hooton et al. 2002; Sujjavanich et al. 2005). Assessment of concrete permeability can be performed using one of the following standard tests: Rapid Chloride Penetration Test (ASTM C1202) and/or Chloride Bulk Diffusion Test (ASTM C1556). For example, Pun (1997) examined the effect of silica fume on the chloride permeability of normal concrete using both alternative test methods. His investigation showed similar trends obtained from both rapid chloride permeability and chloride diffusion test results.

Recently, different methods were developed for predicting the service life of concrete structures exposed to severe environments. These methods identify the total service of concrete structures as two periods, including initiation and propagation periods. Most of these methods calculate the initiation period as a function of the chloride diffusion through the concrete towards the steel bar (Boddy et al. 1999). In these models, a simplified Fickian diffusion approach is applied assuming that the chloride diffusion is the dominant mechanism. In general, the chloride permeability of concrete, in most of the service life prediction methods, is the key factor in measuring the service life time.

Another model was used in developing commercially available software for predicting the service life time (Ehlen et al. 2009). This model is similar to the more complex model proposed by Boddy et al. (1999); however, it accounts for both time and temperature in calculating the coefficient of diffusion of concrete. The initiation period, in this model, is defined as the period of time for sufficient chlorides to penetrate the concrete cover and accumulate at the surface of the embedded steel bars. This sufficient quantity represents the chloride threshold at which corrosion initiates. The model then uses the Fick's second law of diffusion to estimate the initiation time under a number of limitations, regarding the homogeneity of concrete properties and chloride concentrations.

Researchers have focused in measuring the chloride threshold value and the chloride transport rate based on experimental tests and/or field results. For instance, Trejo et al. (2003) proposed a method for experimentally measuring the chloride threshold values for two types of steel reinforcement. In addition, a model for predicting the chloride transport rate was also developed. In this method, the diffusion of chlorides towards the steel bars was accelerated by applying a potential gradient across two electrodes. An anode was embedded at the bar surface, while a cathode was placed in a chloride ion solution of 3.5% concentration. Corrosion initiation was detected by evaluating the polarization resistance of the steel reinforcement by a statistical analysis procedure.

It is not certain, however, whether this threshold value is well representing the sufficient value of chlorides causing corrosion of steel bars. Furthermore, if the chloride permeability is exactly demonstrated by the chloride diffusion coefficient measured as per ASTM C1556. This paper utilizes the results obtained from an electrically accelerated corrosion test to evaluate the current available methods for service life prediction. In addition, it relates different methods for evaluating the chloride permeability of concrete. The significance of this paper is to optimize the use of an accelerated test method to predict the service life time of concrete structures in severe environments.

## **2. Experimental Program**

In this investigation, a self-consolidating concrete (SCC) mixture was used. The mixture was cured for a total period of 28 days under ten different curing techniques yielding ten different concrete qualities. The chloride permeability of each concrete sample was evaluated based on the ASTM standard test methods: Rapid Chloride Penetration Test (ASTM C1202) and Chloride Bulk Diffusion Test (ASTM C1556). The chloride diffusion coefficient at 28 days was also measured for the ten samples based on the ASTM C1556 test method. These coefficients were exploited for predicting the service life time of each concrete sample by applying the Fick's second law of diffusion. For comparison, an accelerated corrosion test was implemented on prism samples casted with the same mixture and cured under the same ten different curing techniques. The samples were casted with the same cover around the embedded steel bar (60 mm). The samples are connected to a DC power supply acting as anode (+), while the steel mesh positioned under the samples as cathode (-). The samples are connected as parallel connections to the circuit board to maintain a constant volt (12 Volts) throughout the whole experiment. The ten samples were totally submerged in a 5% NaCl solution in a container as seen in Figure 1 (Hassan et al. 2009).

The corrosion activity was monitored for the ten samples on a daily basis based on the values of the passed current. In addition, the potential difference between the embedded steel bar and a reference electrode was measured according to ASTM C876. Alternatively, the initiation period was calculated for the ten samples by means of the second Fick's law of diffusion. The results from the accelerated corrosion test were used for validating the results obtained from the second Fick's law of diffusion.

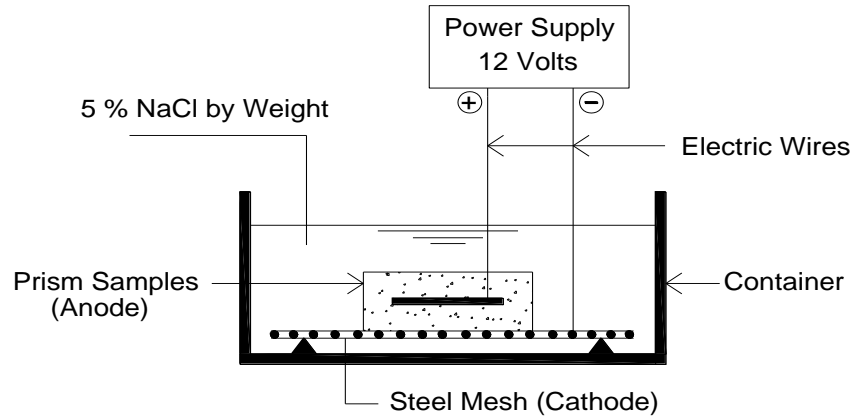


Figure 1: Accelerated Corrosion Test Set-up

## 2.1 Materials and Mixture Design

In this study, type GU Canadian Portland cement similar to ASTM Type I, with a specific gravity of 3.15, was used for the SCC mixture. Natural sand and 10 mm maximum size stone were included as fine and coarse aggregates, respectively. The coarse and fine aggregates each had a specific gravity of 2.70 and water absorption of 1%. A high range water reducer admixture (HRWRA), similar to ASTM Type F (ASTM C494), was applied to attain the required slump flow diameter of SCC mixture. Reinforcing steel bars with the same diameter (20 mm) were used for the ten prism samples. The mixture proportions are shown in Table 1, with an amount of HRWRA added to achieve a slump flow of  $650 \pm 50$  mm.

Table 1: Mixture Proportions for the SCC Mixture

Concrete Type	Cement (kg/m <sup>3</sup> )	W/B	10 mm Stone (kg/m <sup>3</sup> )	Sand (kg/m <sup>3</sup> )	Water (kg/m <sup>3</sup> )	HRWRA (L/m <sup>3</sup> )
SCC	450	0.4	834.0	926.6	180	4.45

## 2.2 Casting, Curing, and Testing of Samples

After mixing of the SCC and obtaining the required slump flow, ten prism samples with a 20 mm steel bar at the center were casted. The samples maintained an equal clear concrete cover from all the sides of 60 mm by means of concrete spacers. The dimensions of all samples were 140 mm x 140 mm x 250 mm. In addition, twenty (100 mm diameter x 200 mm height) cylinders were also casted for chloride permeability testing. The samples (prisms and cylinders) were then cured under ten different curing techniques including air, water curing, heat, and cold temperatures as described in Table 2. The curing techniques are divided into four general categories including air curing at lab temperature (23° C), water curing at 23° C, heated water curing at 50° C, and cold air curing at 3-5° C. Different periods were associated with each curing technique in each curing category as seen in Table 2. At 28 days, all the samples were removed from the different curing spots and left to dry before testing. The cylinders from each curing regime were tested to measure the compressive strength and chloride permeability for each curing system. Meanwhile, the ten alternative prisms were examined by an accelerated corrosion test.

Table 2: Different Curing Techniques

Curing Technique	Description	28-Days $f'_c$ (MPa)
1	28-Days in Air at 23° C	53.16
2	28-Days in Water at 23° C	76.16
3	3-Days in Water then Air both at 23° C	73.33
4	7-Days in Water then Air both at 23° C	75.44
5	3-Days in Water at 23° C then Air at 3-5° C	65.85
6	7-Days in Water at 23° C then Air at 3-5° C	69.21
7	28-Days in Air at 3-5° C	47.45
8	1-Day in Water at 50° C then Water at 23° C	58.91
9	3-Days in Water at 50° C then Water at 23° C	59.38
10	7-Days in Water at 50° C then Water at 23° C	57.88

### 3. Discussion of Test Results

The test results obtained from the rapid chloride penetration and chloride bulk diffusion tests were utilized to derive a relationship between the two test methods. These results and the relationship were then employed to predict the service life time for each prism sample with the same concrete cover. The prediction was performed by using the Fick's second law of diffusion with making some assumptions. To validate these results, the results from the accelerated corrosion experiment were compared for each prism sample under the same conditions.

#### 3.1 Chloride Permeability

At 28 days, the chloride permeability for each curing technique was measured by two different methods as per ASTM C1202 and C1556. For both methods, concrete cylinders with dimensions of 100 x 200 mm were casted and cured as demonstrated above. The first method was the rapid chloride penetration test, in which thick slices of approximately 51 mm were cut from each cylinder. The amount of current passed, through each slice, was measured after 6 hours period of applying a constant potential difference of 60 volts. The total charge passed after this period, in coulombs is related to the resistivity of the concrete to the penetration of chlorides.

The other method (chloride bulk diffusion test), cylinder samples were immersed in 16.5% NaCl solution for a period of 35 days. The cylinder samples were coated with a waterproof epoxy coating on all surfaces except for the top surface. After the immersion period, powder samples are extracted at eight different depths from the exposed surface for analysis of chloride contents. The chloride content profile in the concrete is plotted and used to determine the apparent chloride diffusion coefficient ( $D_a$ ) in  $m^2/sec$  by analysis against the Fick's second law of diffusion (Equation 2). The results from each test method are shown in Table 3.

Table 3: Chloride Permeability of Each Curing System

Curing Technique	RCPT (Coulombs)	$D_a$ ( $m^2/sec$ )
1	3000	9.33 E-12
2	2072	7.52 E-12
3	2130	8.86 E-12
4	2100	8.32 E-12
5	2596	7.99 E-12
6	2432	7.85 E-12
7	3120	9.62 E-12
8	3093	1.22 E-11
9	3633	1.50 E-11
10	3700	1.80 E-11

### 3.1.1 Effect of Different Curing Techniques on Chloride Permeability

The results, presented in Table 3, showed that different curing techniques had a significant effect on both the RCPT and chloride diffusion coefficients. The results from the RCPT test ranged between 2072 and 3700 which classified as moderate penetrability as per ASTM C1202. The sample with the minimum permeability was number 2, which was cured at water for 28 days at 23° C. On the other hand, the maximum permeability was associated with the sample number 10, which was cured in heated water at 50° C for a period of 7 days. Furthermore, samples number 5, 6 and 7 had an average permeability of 2716 which was lower than the air-cured sample 1. It can be also seen from Table 3 that the water-cured samples (2, 3 and 4) had almost similar RCPT permeability. However, the increase in the water-curing period at 23° C slightly decreased the chloride permeability. In addition, when samples 5 and 6 were subsequently cured in air, after water curing periods, the permeability was increased. Ultimately, when sample 7 was cured at cold air (3-5° C), the chloride permeability was higher than the normal air-cured sample (1). It is obvious that heat-cured samples (8, 9 and 10) exhibited the maximum average chloride permeability.

Alternatively, the results from the chloride diffusion test also indicated a significant effect of curing on the chloride diffusion coefficient. It is again clear from Table 3 that a minimum chloride diffusion coefficient of 7.52E-12 m<sup>2</sup>/sec was associated with the mixture with minimum RCPT coulombs (2). Moreover, a maximum value of 1.8E-11 m<sup>2</sup>/sec was obtained from sample number 10. In fact, the effect of using different curing techniques on the chloride diffusion coefficients yielded an identical effect of that on the RCPT permeability (see Figure 2).

### 3.1.2 Relationship between RCPT and Chloride Diffusion Tests

It is clear from Figure 2 that the relation between the two alternative methods, for measuring chloride permeability, is almost linear. Using this linear relationship, the diffusion coefficient can be estimated by substituting the RCPT value in Equation 1. It should be noted that this equation is based on certain parameters of the SCC mixture. Even so, it can provide estimation for the chloride permeability after six hours only, instead of 35 days.

[1] Chloride Diffusion Coefficient  $D_a$  (m<sup>2</sup>/sec) = - 2.4718 E-12 + 4.9208 E-15 \* RCPT (Coulombs) [R<sup>2</sup> = 0.67]

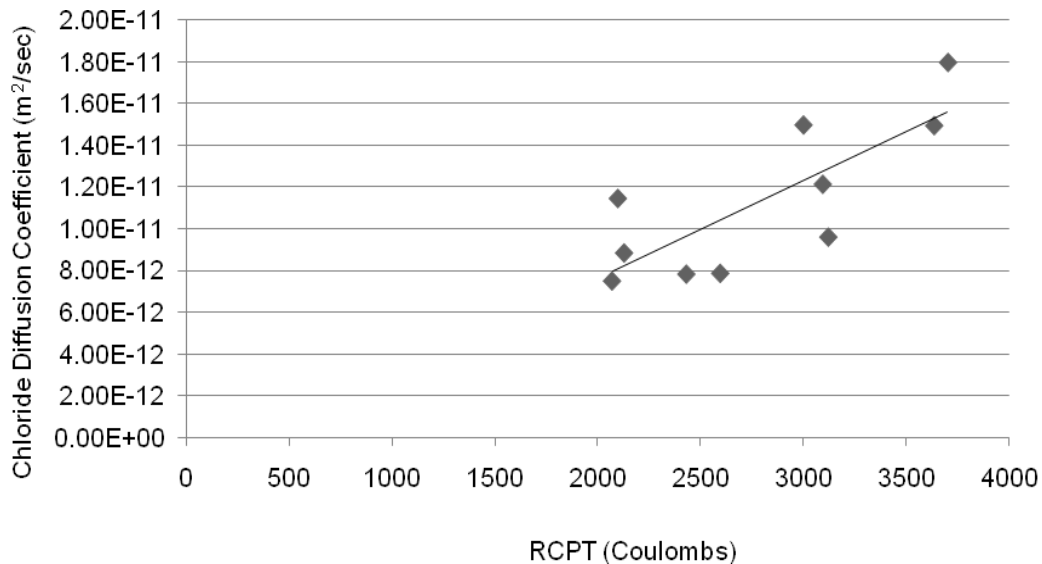


Figure 2: Relationship between RCPT and Chloride Diffusion Tests

### 3.2 Service Life Time Prediction

After measuring the chloride diffusion coefficients for each curing technique, the following assumptions were made to predict the service life time for the ten tested samples:

- The structure has a clear concrete cover of 60 mm,
- The chloride threshold value is 0.05% (% weight of concrete),
- The chloride diffusion is the dominate mechanism and is governed by the Fick's second law of diffusion in the differential Equation 2;

$$[2] \quad dC/dt = D_a * (d^2C/dx^2)$$

Where:  $C$  = the chloride content,  $D_a$  = the apparent diffusion coefficient,  $x$  = the depth from the exposed surface, and  $t$  = time.

- The chloride diffusion coefficients showed in Table 3 (at 28 days) decreases periodically as a function of time because of the cement hydration process. As a result, the chloride diffusion should be calculated at different time periods using the following equation:

$$[3] \quad D(t) = D_{ref} * (t_{ref}/t)^m$$

Where:  $D(t)$  = diffusion coefficient at time  $t$ ,  $D_{ref}$  = diffusion coefficient at time  $t_{ref}$  (28 days), and  $m$  = diffusion decay index (Constant value of 0.44 for the present SCC mixture).

- The surface chloride concentration ( $C_s$ ) of the simulated structure had reached the maximum value of 0.8% weight of concrete (or more) at the start time of chloride diffusion.

The solution for estimating the time of corrosion initiation was implemented using a finite difference application of Equation 2. The values of chloride diffusion coefficient were varied at different time steps, until the value of chloride concentration reaches the chloride threshold value. At this stage, the time was reported which indicated the corrosion start for each sample as seen in Table 4. It should be mentioned that the initiation period calculated herein was based on assuming the maximum surface chloride concentration (0.8%) was accumulated previously. This assumption is not real for actual structures, as it may take years for chlorides to build up at the surface of the exposed structure. However, this assumption was made to be able to compare the initiation period, calculated by the Fick's second law of diffusion, by the results from the accelerated corrosion experiment.

Table 4: Predicted Corrosion Initiation Period for Each Curing Technique

Curing Technique	Predicted Initiation Period (Years)
1	2.0
2	3.8
3	3.2
4	3.4
5	3.5
6	3.6
7	2.6
8	1.8
9	1.3
10	1.0

### 3.2.1 Effect of Different Curing Techniques on Initiation Period

It is clear from Table 4 that different service life time periods were warranted for different curing techniques. The samples had the same cover thickness and concrete type; however, different curing methods were made for each sample. Therefore, the only difference in their service life time periods was attributed to the different diffusion coefficients between the ten samples. For instance, an identical initiation period was obtained from samples 1 and 9, as they had approximately the same chloride diffusion coefficients.

The sample with the minimum chloride permeability (2) exhibited the longest initiation period (3.8 years), as seen in Table 4. Similarly, the first corrosion onset (1.0 years) was associated with the sample with the highest permeability (10). In general, a linear relationship was obtained between both the chloride permeability and initiation period. These results were attributed to the presumed assumptions, especially assuming the chloride diffusion is the dominant mechanism. As a result, experimental validation of these results was needed to overcome this limitation.

### 3.3 Accelerated Corrosion Test

By reviewing the results from the initiation periods, it was proved that corrosion requires a relatively long period to start. For this reason, an accelerated corrosion was performed on ten identical samples by the procedure described in Section 2. The corrosion activity of the ten samples was monitored by means of electrical current measurements and half-cell potentials (as per ASTM C876). Figure 3 demonstrates the general trend for the current versus time and half-cell potentials versus time relationships, for sample number 2, as an example. The time of corrosion onset was detected at the point of the jump (sudden increase) in the current reading. This point was also evaluated based on the readings of the half-cell potential test. The half-cell readings indicate a greater than 90% probability of reinforcing steel corrosion is occurring, if the measured potentials for the sample are less than  $-350$  mV.

By reviewing the current and half-cell readings, the initiation of corrosion was identified for each sample from 1 to 10 and recorded as demonstrated in Table 5. It should be noted that almost identical trends were obtained from both current and half-cell measurements versus time. These results showed a minimum initiation period of 18 days associated with sample number 10, which exhibited the maximum chloride permeability. On the other hand, the maximum period of 53 days was obtained from sample number 2, as expected. This sample had a superior performance owing to the minimum chloride permeability which increased the resistance to corrosion. This finding revealed a similar trend from the service life prediction model used in section 3.2 and presented in Table 4. Nevertheless, the results obtained from the accelerated corrosion test can not be compared with the actual initiation period, which requires years.

Table 5: Accelerated Corrosion Initiation Period for Each Curing Technique

Curing Technique	Passing Current (mA)	Half-Cell Potentials (mV)	Accelerated Initiation Period (Days)
1	19.3	-440	25
2	21.9	-352	53
3	16.6	-377	50
4	21.1	-350	52
5	21.7	-401	46
6	24.5	-392	43
7	19.4	-357	42
8	28.1	-404	21
9	27.8	-357	20
10	29.3	-355	18

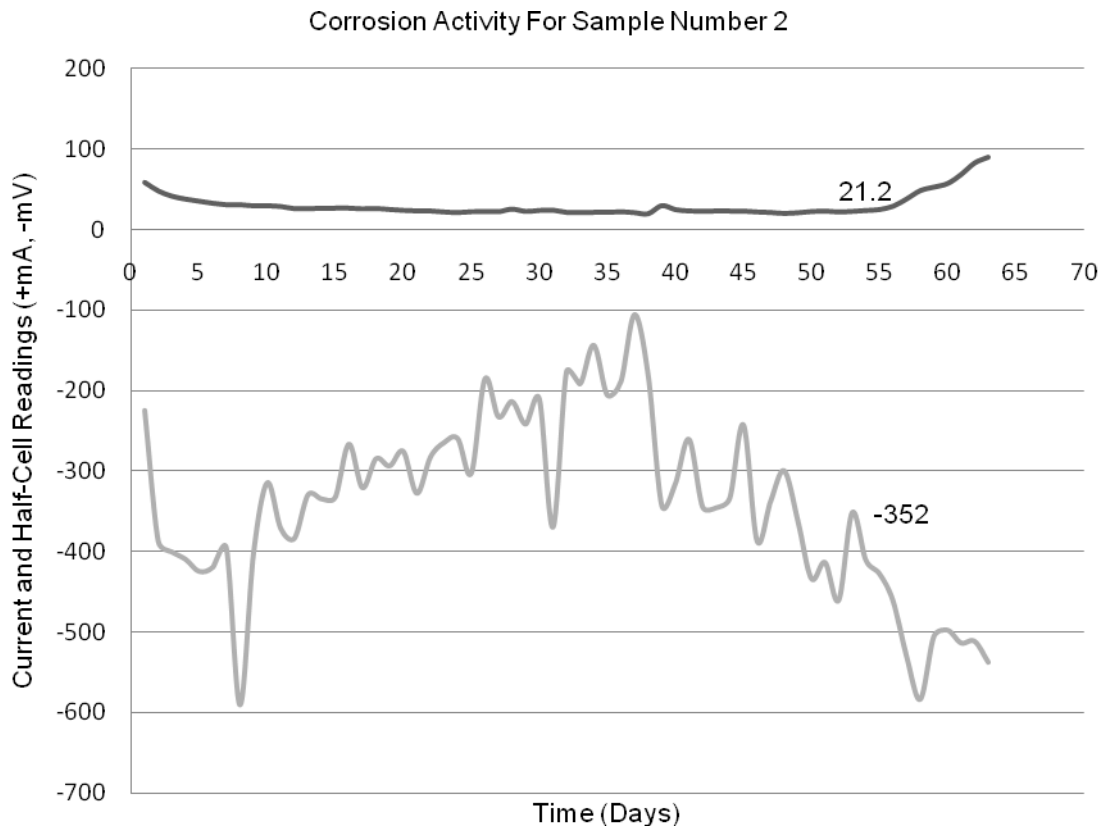


Figure 3: Time versus Current and Half-Cell Relationships for Sample 2

Based on this method, the corrosion initiation was detected as seen in Figure 3, as an example for sample number 2. It is clear that corrosion started just after reaching a minimum value of the passing current (21.2), and a sudden increase can then be seen after this point from the top part of Figure 3. This point was assured by obtaining the half-cell reading greater than -350, which indicated that a probability of corrosion activity was greater than 90%. The half-cell readings versus time showed a linear relationship between the amount of passing current and the corrosion potential difference. Furthermore, the half-cell readings greater than -350 were followed by significantly higher negative readings, as presented in the bottom part of Figure 3. Similarly, the initiation period, current reading, and half-cell reading were measured and reported for all samples from 1 to 10, as seen in Table 5.

### 3.3.1 Effect of Different Curing Techniques on the Corrosion Activity

It can be seen from Table 5 that the different curing techniques had a significant effect on current readings, half-cell readings, and initiation period. It is clear that normal water-cured samples (2, 3, and 4) had the maximum times to corrosion higher than both cold air-cured (5, 6, and 7) and heated water-cured (8, 9, and 10) samples. In addition, the normal temperature air-cured sample (1) had a longer initiation period (25 days) than all heated water-cured samples (18-21 days). However, the difference between normal water-cured samples was not significant, which ranged between 50 and 53 days. Identically, the difference between cold air-cured samples was between 42 and 46, and between heated water-cured samples, was 18 and 21 days. These ranges were attributed to the fact that these samples had almost the same chloride permeability, which represents the concrete resistivity to corrosion. It should be also mentioned that the ten samples had exactly the same conditions in the accelerated corrosion test.



### 3.3.2 Comparison between the Initiation Periods from Fick's Law and the Accelerated Corrosion Test

To be able to compare between the accelerated corrosion test and the predicted values from the Fick's law, the results were normalized as a percentage of the maximum period obtained from sample number 2. The results from the accelerated corrosion test are described as a percentage of days, while the results from the Fick's law are shown as a percentage of years (See Figure 4). It is obvious from Figure 4 that the differences between both methods of prediction were almost non-significant. Even though, some samples (for example, 3 and 6) exhibited higher differences which may be attributed to the non-homogeneity between the concrete tested in the accelerated corrosion and in chloride diffusion tests.

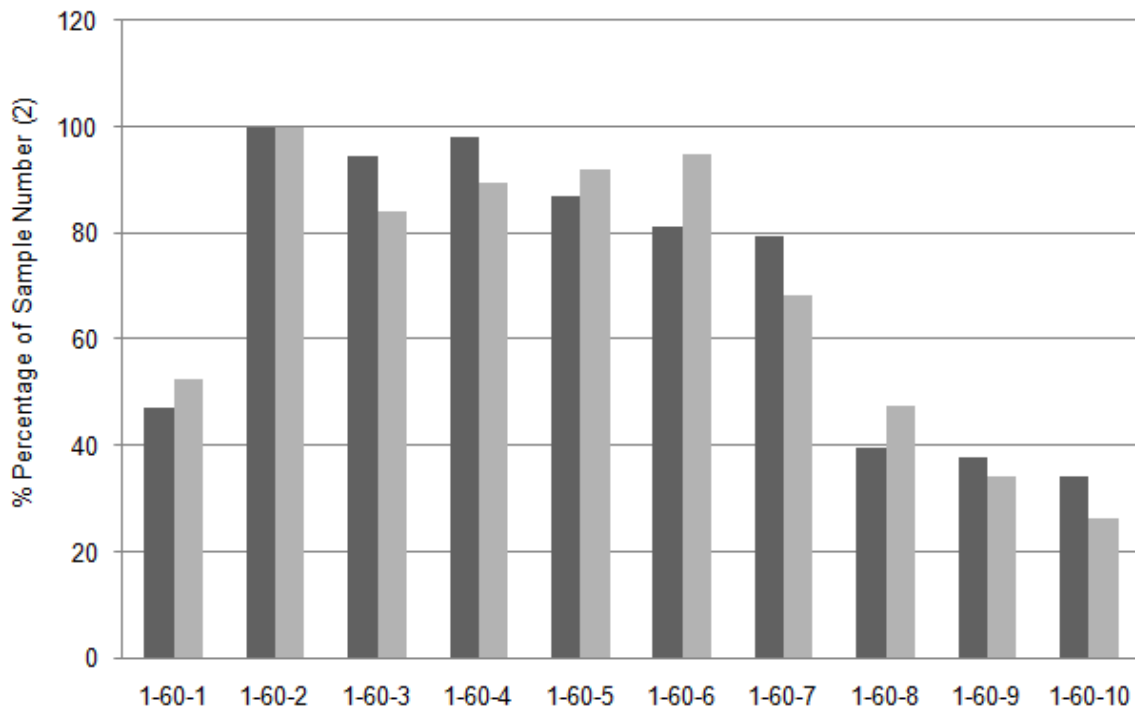


Figure 4: Initiation Periods from Fick's Law and the Accelerated Corrosion Test

## 4. Conclusions

In the present paper, SCC mixture was cured under ten different curing techniques yielding ten different concrete samples with different qualities. These samples were then tested to evaluate the chloride permeability by two standard test methods in order to calculate their diffusion coefficients. Using these coefficients, the service life time was predicted for each sample, using the Fick's second law of diffusion. Finally, an accelerated corrosion test was implemented to validate the results. By reviewing all these results, the following conclusions were obtained:

- The relationship between the RCPT values and chloride diffusion coefficients was almost linear.
- The use of longer periods of water curing (at 23° C) decreased the chloride permeability and increased the time to corrosion obtained from both the accelerated corrosion test and Fick's second law of diffusion. On the contrary, applying heated water curing (at 50° C) for longer periods maximized the permeability and reduced the corrosion initiation period.

- Subsequent curing at cold air (at 3-5° C) for a longer duration negatively affected the chloride permeability, thus decreasing the time for corrosion onset.
- The water curing for a period of 28-days (at 23° C) proved to be the best curing system.
- The corrosion initiation periods from the accelerated corrosion test mostly matched the results from the Fick's second law of diffusion, for counterpart samples.
- A linear relationship was warranted between the electrical current measurements and the half-cell potential values in the accelerated corrosion test.
- A value of half-cell potential greater, in negative, than -350 mV indicated the corrosion initiation on the accelerated corrosion experiments.

## References

- A.M. Boddy, M.D.A. Thomas, and R.D. Hooton, An Overview and Sensitivity Study of a Multi-Mechanistic Chloride Transport Model, *Cement and Concrete Research*, V. 29, 1999: pp. 827-837.
- A.A.A. Hassan, K.M.A. Hossain, M. Lachemi, Corrosion resistance of self-consolidating concrete in full-scale reinforced beams, *Cement & Concrete Composites*, V. 31, 2009: pp. 29-38.
- ASTM C1202-97, Standard Test Method for Electrical Indication of Concrete's Ability to Resist Chloride Ion Penetration, *ASTM International*, West Conshohocken, 1997.
- ASTM C876-91, Standard Test Method for Half-Cell Potentials of Uncoated Reinforcing Steel in Concrete, *ASTM International*, West Conshohocken, 1991.
- ASTM C1556-11a, Standard Test Method for Determining the Apparent Chloride Diffusion Coefficient of Cementitious Mixtures by Bulk Diffusion, *ASTM International*, West Conshohocken, 2011.
- David Trejo and Radhakrishna G. Pillai, Accelerated Chloride Threshold Testing: Part I - ASTM A 615 and A 706 Reinforcement, *ACI Materials Journal*, V. 100, No. 6, 2003: pp. 519-527.
- Mark A. Ehlen, Michael D.A. Thomas, and Evan C. Bentz, Widely Used Software Helps Assess Uncertainties in Concrete Service Life and Life-Cycle Costs, *ACI Concrete international*, 2009: pp. 41-46.
- Pierre Che Ho Pun, Influence of Silica Fume on Chloride Raistance of Concrete, M.A.Sc. Thesis 1997, Department of Civil Engineering, Univensty of Toronto.
- R. Douglas Hooton, Mette R. Geiker, and Evan C. Bentz, Effects of Curing on Chloride Ingress and Implications on Service Life, *ACI Materials Journal*, V. 99, No. 2, 2002: pp. 201-206.
- Suvimol Sujjavanich, Voradej Sida, and Prasert Suwanvitaya, Chloride Permeability and Corrosion Risk of High-Volume Fly Ash Concrete with Mid-Range Water Reducer, *ACI Materials Journal*, V. 102, No. 3, 2005: pp. 177-182.